Ecology, 87(6), 2006, pp. 1478–1488

THE SCALE TRANSITION: SCALING UP POPULATION DYNAMICS WITH FIELD DATA

BRETT A. MELBOURNE[1,3] AND PETER CHESSON[2]

[1]*Center for Population Biology, University of California, Davis, California 95616 USA*
[2]*Department of Ecology and Evolutionary Biology, University of Arizona, Tucson, Arizona 85721 USA*

Abstract. Applying the recent developments of scale transition theory, we demonstrate a systematic approach to the problem of scaling up local scale interactions to regional scale dynamics with field data. Dynamics on larger spatial scales differ from the predictions of local dynamics alone because of an interaction between nonlinearity in population dynamics at the local scale and spatial variation in density and environmental factors over the regional population. Our systematic approach to scaling up involves the following five steps. First, define a model for dynamics on the local spatial scale. Second, apply scale transition theory to identify key interactions between nonlinearity and spatial variation that translate local dynamics to the regional scale. Third, measure local-scale model parameters to determine nonlinearities at local scales. Fourth, measure spatial variation. Finally, combine nonlinearity and variation measures to obtain the scale transition. Using field data for the dynamics of grazers and periphyton in a freshwater stream, we show that scale transition terms greatly reduce the growth and equilibrium density of the periphyton population at the stream scale compared to rock scale populations, confirming the importance of spatial mechanisms to stream-scale dynamics.

Key words: *heterogeneity; nonlinear dynamics; scale; spatial ecology.*

INTRODUCTION

A central problem in spatial ecology is predicting large-scale population dynamics from small-scale processes, and understanding why large-scale outcomes contradict small-scale trends. Development of theory in this area over several decades has been substantial but has outpaced application to field systems (Steinberg and Kareiva 1997). Scale transition theory (Chesson 1978, 1996, 1998*a*, *b*, Chesson et al. 2005) is a powerful new approach to understanding spatiotemporal dynamics that leads naturally to empirical assessment. Here, we apply scale transition theory to field data for stream periphyton and grazers, to predict large-scale dynamics and to quantify mechanisms that drive the most important changes to population dynamics on the larger scale.

Scale transition theory shows that the most important changes in dynamics at the larger scale can be attributed to interactions between local-scale nonlinear population dynamics and spatial variation in either population density or the physical environment (Chesson 1978, 1996, 1998*a*, *b*, Chesson et al. 2005). Large-scale dynamical outcomes that contradict small-scale predictions can be traced to such interactions in a wide range of spatiotemporal models, including changes to stability, persistence, coexistence, and carrying capacity (De Jong 1979, Ives 1988, Hassell et al. 1991, Bolker and Pacala 1997, 1999, Pacala and Levin 1997, Chesson 2000, Snyder and Chesson 2003, 2004). As it is straightforward to quantify local nonlinearities and spatial variation, it is possible to measure their theoretically predicted interaction for specific field systems, as we have shown with simulated data (Melbourne and Chesson 2005). If spatial models are correct in their predictions that variation in environmental conditions and population densities explain important dynamical phenomena, such as stability and coexistence, then a properly measured interaction should be of the right magnitude and sign, and should change with system parameters in a way that explains the relevant phenomenon. In this study, we do not focus on a specific dynamical phenomenon. Instead, we provide proof of concept by measuring the interaction between nonlinearity and variation in a consumer-resource system and determining its effect on resource dynamics at the larger scale.

Interactions between individuals, both within and between species, invariably lead to nonlinear dynamics, which can be defined by a model for local dynamics with parameters that can be measured from field data. According to scale transition theory, when densities vary in space, and in some cases when environmental factors vary in space, large-scale dynamics differ from the predictions of local-scale dynamics due to interactions between spatial variation and nonlinearities in local dynamics (Chesson et al. 2005). Scale transition theory identifies these critical interactions and defines the measures of variation needed from field data to scale up. The theory then shows how these measures of variation

Manuscript received 28 April 2005; revised 21 November 2005; accepted 30 November 2005. Corresponding Editor: A. M. de Roos.
[3] E-mail: bamelbourne@ucdavis.edu

combine with measures of nonlinearity to determine the change in dynamics from the local to the regional scale, that is, the scale transition. Hence, a systematic approach to studying the scale transition has five steps: (1) define a model for dynamics on the local spatial scale, (2) apply scale transition theory to identify key interactions between nonlinearity and spatial variation that translate local dynamics to the regional scale, (3) measure local-scale model parameters to determine nonlinearities at local scales, (4) measure spatial variation, (5) combine nonlinearity and variation measures to obtain the scale transition. We describe the first two steps here, applied to stream periphyton and its invertebrate grazers. The remaining steps are described in *Methods* and *Results*.

Model for dynamics on the local scale

We distinguish two scales: the rock scale, corresponding to the upper surface (approximately 10–20 cm diameter) of a rock on the stream bed; and the stream scale (approximately 5 km length of stream). We shall consider the local scale to be the rock and the regional scale the stream (see Chesson 1996 and 1998*a* for how to choose scales). We begin by formulating a general model for local dynamics, with submodels for specific components to be determined later. At the rock scale, periphyton dynamics are determined by three processes: periphyton growth, consumption by grazers, and dispersal of periphyton to and from the rock, such that

$$\frac{dR_x}{dt} = g(R_x) - f(R_x)C_x + I_{\mathrm{R},x} - E_{\mathrm{R},x} \qquad (1)$$

where R is resource density (periphyton biomass per unit area), t is time, x indexes rocks, C is consumer density (grazer biomass per unit area), and subscript R denotes resource. The function $g(R)$ describes periphyton growth rate (biomass per unit area per unit time) as a function of periphyton density, and $f(R)C$ describes the rate of periphyton consumption by grazers, where $f(R)$ is the functional response of a grazer. In writing consumption as $f(R)C$, we assume that grazer consumption is proportional to grazer density, which means that grazers do not interact with each other directly through interference but only indirectly by consuming periphyton, a standard assumption (Nisbet et al. 1997). Periphyton dispersal to and from rock x is modeled by the generic functions $I_{\mathrm{R},x}$ (immigration) and $E_{\mathrm{R},x}$ (emigration), to which any set of dispersal rules could be assigned, provided that dispersal mortality is factored into the growth rate terms (Chesson 1998*a*). For example, periphyton immigration rate, I_{R}, at rock x might depend on the output from nearby rocks and the velocity and direction of stream currents. A model for grazer dynamics on rock x is

$$\frac{dC_x}{dt} = \Big(cf(R_x) - m\Big)C_x + I_{\mathrm{C},x} - E_{\mathrm{C},x} \qquad (2)$$

where c is the conversion efficiency of grazers, m is grazer mortality, and grazer movement is modeled by the generic functions $I_{\mathrm{C},x}$ and $E_{\mathrm{C},x}$. Thus, a model for the local dynamics of periphyton and grazers consists of the coupled Eqs. 1 and 2. To match the time scale of field experiments (i.e., two to three weeks), we reformulate the model for grazer dynamics (Eq. 2) to a short time scale, over which the net gain in grazer density due to the consumption of periphyton is negligible (Nisbet et al. 1997). Thus, we set $(cf(R_x) - m)C_x = 0$, since the local dynamics of grazers mostly reflects movement to and from the rock. For example, movement might be a result of foraging decisions made by individual grazers, or a response to environmental conditions, stream flow, or predators at the rock. To fully specify the model, we need to specify submodels for $g(R)$ and $f(R)$ but for now we leave the model in its general form and proceed to scale up. As we will show, there is no need to specify the periphyton dispersal and grazer movement functions.

Scale transition theory: nonlinearity-variation interactions

We wish to scale up from the local scale of a rock to the regional scale of a stream, where rocks are now linked by dispersal of periphyton and movement of grazers. In general, population densities on a large scale can be expressed as averages of densities on smaller scales (Chesson 1998*a*). Here, the regional density is the average of the rock-scale densities, and so the regional dynamics are obtained by averaging both sides of Eqs. 1 and 2:

$$\frac{d\overline{R}}{dt} = \overline{g(R) - f(R)C + I_{\mathrm{R}} - E_{\mathrm{R}}} = \overline{g(R)} - \overline{f(R)C} + \overline{I_{\mathrm{R}}} - \overline{E_{\mathrm{R}}}$$

$$= \overline{g(R)} - \overline{f(R)C}$$

$$\frac{d\overline{C}}{dt} = \overline{I_{\mathrm{C}} - E_{\mathrm{C}}} = \overline{I_{\mathrm{C}}} - \overline{E_{\mathrm{C}}} = 0 \qquad (3)$$

where the overbars indicate the spatial average. Thus, the rate of change in periphyton density at the regional scale is the average of the local rock-scale functions for growth, consumption, and dispersal. As averages are additive, the regional average simplifies to the separate averages for growth, consumption, and dispersal (Eq. 3). At the stream scale, the system can be considered effectively closed (as defined by Chesson 1996). For example, grazers might move extensively within a stream by a range of dispersal mechanisms (Hershey et al. 1993) but there is very little movement of larval grazers between streams (Downes and Keough 1998). Between-catchment migration by adults is not relevant on the short time-scale considered here. Thus, individuals that leave a rock enter another rock within the stream, so that the total leaving rocks is equal to the total entering rocks (i.e., $\overline{I} - \overline{E} = 0$), while we assume that dispersal mortality is built into the local functions. Regardless of the exact mode of dispersal, the dispersal functions disappear at the regional scale (Eq. 3).

To find the scale transition, we express the regional dynamics as being composed of the local dynamics plus scale transition terms that account for scaling up (see Appendix A):

$$\frac{d\overline{R}}{dt} = \underbrace{g(\overline{R}) - f(\overline{R})\overline{C}}_{\text{mean-field model}} + \underbrace{T_g}_{\text{a}} - \underbrace{T_f\overline{C}}_{\text{b}} - \underbrace{T_{fC}}_{\text{c}}, \qquad (4)$$

where T_g and $T_f\overline{C}$ are scale transition terms arising respectively from nonlinearity in periphyton growth and nonlinearity in the consumer functional response. The final scale transition term, T_{fC}, arises because the consumption rate is a product of the consumer functional response and consumer density. The product of two variables is a nonlinearity in two dimensions (see Chesson et al. 2005). Here, the two dimensions are the functional response, $f(R)$, and the consumer density, C. The key concept in Eq. 4 is that the mean-field model represents local dynamics: it is the model that would apply at the rock scale in the absence of migration between rocks at different densities. In this light, the scale transition is the difference between regional and local dynamics (Chesson et al. 2005). The total scale transition thus equals the sum of the three scale transition terms (a–c) to the right of the mean-field model.

The scale transition terms in Eq. 4 are a consequence of nonlinear averaging: the average of the function is generally different from the function of the average when the function is nonlinear. The mean-field model is the function of the average, so the scale transition terms (a–c) quantify the difference between the average of the function and the function of the average. Special cases of nonlinear averaging in ecology that have been discussed previously are Jensen's inequality (Chesson 1981, 1991, Ruel and Ayres 1999), and the idea of the "fallacy of the averages" (Welsh et al. 1988). The importance of nonlinear averaging to spatial ecology was first discussed by Chesson (1978) and a precursor can be found in Lloyd's mean crowding (Lloyd 1967).

The scale transition terms in Eq. 4 can be understood in terms of interactions between nonlinearity and spatial variation, from general scale transition formulae derived in Chesson et al. (2005). Applied here, the general formulae show that T_g is approximately $\frac{1}{2}g''(\overline{R})\mathrm{Var}(R)$ and T_f is approximately $\frac{1}{2}f''(\overline{R})\mathrm{Var}(R)$. In both of these cases, the second derivative defines the nonlinearity of the function, which is multiplied by the spatial variance of periphyton between rocks. The final scale transition term T_{fC} exactly equals $\mathrm{Cov}(f(R),C)$, the covariance in space between the functional response and consumer density (Appendix A). This covariance can be approximated as $f'(\overline{R})\mathrm{Cov}(R,C)$ (Chesson et al. 2005), where $\mathrm{Cov}(R,C)$ is the covariance between periphyton and grazer density over rocks (Appendix A). Putting them all together we obtain the full approximation for grazer dynamics:

$$\frac{d\overline{R}}{dt} \approx \underbrace{g(\overline{R}) - f(\overline{R})\overline{C}}_{\text{mean-field model}} + \underbrace{\tfrac{1}{2}g''(\overline{R})\mathrm{Var}(R)}_{\text{a}} - \underbrace{\tfrac{1}{2}f''(\overline{R})\mathrm{Var}(R)\overline{C}}_{\text{b}} - \underbrace{f'(\overline{R})\mathrm{Cov}(R,C)}_{\text{c}}. \qquad (5)$$

The approximation shows that, as products of measures of nonlinearity and measures of spatial variation, the scale transition terms represent interactions between nonlinear dynamics and spatial variation.

Given the importance of nonlinearities, it is worthwhile seeing how each arises. Periphyton growth at the local scale, $g(R)$, would only be linear if there were no density dependence in growth. However, competition for resources (e.g., light) within the periphyton biofilm is a well-established phenomenon (Hill and Boston 1991, Hill 1996) and ensures that $g(R)$ is nonlinear, for example, as in the logistic model. Nonlinearity would occur with light as a resource because, as the periphyton grows thicker, lower-lying cells would be increasingly shaded by cell layers above. For the functional response of grazers, $f(R)$, local nonlinearities might result from a handling time requirement or an attack rate that varies with periphyton density, for example, as in a classic type II or type III functional response (Holling 1959). The third scale transition term (c) also results from an interaction between nonlinearity and spatial variation due to the two-dimensional nonlinearity of periphyton and grazer density. This nonlinearity arises directly because grazers eat periphyton, thus causing the functional response and consumer density to enter the consumption rate as a product.

The scale transition terms can be thought of as quantifying separate spatial mechanisms. To analyze the importance of spatial mechanisms to dynamics, we consider the magnitude and sign of the scale transition terms relative to the mean-field model and to each other. Depending on the sign of the second derivatives $g''(\overline{R})$ and $f''(\overline{R})$, which are determined by whether each function is concave down (negative second derivative) or concave up (positive second derivative), the first two scale transition terms (a and b) may work either in opposing directions, thus moderating the effect of variation, or in the same direction, thus compounding the effect of variation on stream-scale dynamics. The effect of spatial variation in grazer density enters only through spatial covariation with periphyton density and depends on the sign and magnitude of the spatial covariance between grazer and periphyton density (c). Spatial variance and covariance can arise in many ways and are sometimes determined by the details of dispersal. Thus, the effect of different dispersal modes on stream-scale dynamics is accounted for in the scale transition terms in which the variance and covariance appear. As the scale transition terms are responsible for changing dynamics at the larger scale of the stream, they

TABLE 1. Alternative models for periphyton growth and removal rate by grazers

Name	Model	Parameters
Models for periphyton growth		
Resource gradient†	$g(R) = \frac{P_0}{\rho}(1 - e^{-\rho R}) - mR$	P_0, photosynthetic rate at periphyton surface ρ, determines rate of decline of photosynthesis with depth in the periphyton m, rate of density loss per unit of density, due to respiration and metabolism
Logistic	$g(R) = rR\left(1 - \frac{R}{K}\right)$	r, density independent growth rate K, density at equilibrium
Exponential growth	$g(R) = rR$	r, density independent growth rate
Constant accumulation	$g(R) = \alpha$	α, accumulation rate
Models for removal rate of periphyton by grazers		
Type II	$f(R)C = \frac{aR}{1 + ahR}C$	a, attack rate of the grazer h, handling time of the grazer
Type III	$f(R)C = \frac{bR^2}{1 + bhR^2}C$	b, linear parameter for the attack rate of the grazer h, handling time of the grazer
Linear increase	$f(R)C = aRC$	a, attack rate
Saturated	$f(R)C = cC$	c, constant removal rate

† The resource gradient model is derived in Appendix B.

are key quantities that can be measured in the field to provide a general test of spatial mechanisms. We measure these quantities for periphyton and grazers by fitting models to describe nonlinearities at the rock scale, and using appropriate sampling and estimation methods to measure spatial variation. We show that the combined magnitude of the scale transition terms is sufficient to change dynamics at the larger scale.

METHODS

Study system and field site

The Bimberamala and Yadboro Rivers are fourth-order streams (sensu Strahler 1952), part of the Clyde River system in southeastern New South Wales, Australia (35°23′ S, 150°10′ E). The stream bed consists of rounded cobbles 10–20 cm in diameter. The mean depth of experimental sites was 11 cm, and mean stream velocity was 4.5 cm/s. Periphyton assemblages were dominated by diatoms and green algae. Periphyton was consumed by grazing invertebrates, mainly the aquatic larvae of caddisfly (Trichoptera), mayfly (Ephemeroptera), and waterpenny (Coleoptera: Psephinidae) species.

Measuring nonlinearity: local submodels

To measure local nonlinearities, we specified alternative models for the growth and foraging functions in Eq. 1, and fitted these to rock-scale data from a field experiment to test for differences between alternative models. We specified four alternative models for periphyton growth and four alternative models for the removal rate of periphyton by grazers (Table 1). As discussed, these models ought not be linear but we included linear models among the alternatives as a check on the discriminatory power of the data.

Grazer exclusion experiment

The data for fitting growth and foraging models consisted of initial and final measurements of periphyton density over 25 days, with and without grazers. We set up 40 randomly located pairs of rocks in the stream, each pair having one rock with grazers excluded by an electric pulse (Brown et al. 2000) and the other rock freely accessible to grazers. Rocks in a pair were 50 cm to 1 m apart. Pairs of rocks were arranged in the stream in a hierarchical design described in *Estimation of variance and covariance*. A periphyton sample (2.4 cm diameter) was removed randomly from the top surface of each rock using a standard sampler (Flower 1985). The sample was taken immediately before implementing grazer exclusion. A second sample was taken 25 days later, 5 cm from the initial sample, in a random direction. Periphyton biomass was measured as ash free dry weight using a standard procedure (Britton and Greeson 1989:129–130). Grazers were sampled at the time of the final periphyton sample. Rocks were collected from the stream bed into a net and, after first taking the periphyton sample, grazers were removed with a brush (following Downes et al. 1993). Grazer density was measured as dry mass per square centimeter of exposed rock surface area (following Doeg and Lake 1981, Graham et al. 1988), where dry mass was

estimated from individual body lengths using allometric relationships (Smock 1980, Meyer 1989, Towers et al. 1994).

Selection and parameter estimation of local models

We obtained maximum likelihood estimates of rock-scale model parameters, where each model (Table 1) was fitted to the final periphyton density assuming lognormal errors. The predicted final density was obtained by integrating over time starting from the initial density. We inspected likelihood profiles to ensure that parameters were well defined by the data. Models for periphyton growth, $g(R)$, were fitted to the periphyton data from the ungrazed rocks. Models for the removal rate of periphyton, $f(R)C$, were fitted to the periphyton data from the grazed rocks with grazer density as an independent variable, and with $g(R)$ set to the best-fitting model estimated previously from the ungrazed data. To determine which of the alternative models was most consistent with the data, we used the Akaike information criterion (AIC) (Akaike 1992).

The fitting method just described assumes that all of the error in the model fit is in the final density, and that initial density is measured without error. Since there is observation error in the initial density, the parameter estimates are biased (Carroll et al. 1995). To reduce bias in the parameter estimates for the best-fitting models, we used the simulation-extrapolation (SIMEX) method to adjust maximum likelihood estimates (Cook and Stefanski 1994, Stefanski and Cook 1995), based on the observation error estimated separately by variance components analysis. We used C++ for all of the numerical work described here.

While taking the grazer samples, we discovered that the sampling technique did not efficiently capture an abundant grazer in the Yadboro River. This was a large-bodied (2–3 cm) freshwater shrimp (Atyidae). These grazers were most active at night and were conspicuous by spotlight at many sites on the Yadboro River, yet rare in our samples. They were rarely observed in the Bimberamala River. Since we were not able to estimate the density of this species, we fitted grazer models only to the data from the Bimberamala River and tributaries ($n = 20$).

Estimation of spatial variance and covariance

We used a hierarchical sampling design to measure the spatial variance components of periphyton density and the components of spatial covariance for periphyton and grazer density. The hierarchical sampling design included five spatial scales. There were two catchments at the largest scale (stream scale). Within each stream, there were three sections of stream, each 1.6 km long (reach scale). There were three or four sites located randomly within each reach, such that there were 20 sites in total. Each site was a 10-m stream length (site scale). Within each site, two 1-m^2 plots were randomly located on the stream bed (plot scale). Within each plot, two rocks were selected as experimental units as described in *Grazer exclusion experiment* (rock scale). In the entire experiment, there were 80 rocks, 40 with grazers excluded and 40 freely accessible to grazers.

Spatial variance components were estimated using restricted maximum likelihood (REML; e.g., Searle et al. 1992), after first transforming periphyton density to the natural-logarithm scale. REML was used because the design was hierarchical and not all units on all scales were measured. Exploratory analyses (e.g., theoretical quantile–quantile plots) implied that periphyton density was well fitted by a lognormal distribution (Chambers et al. 1983). Variances were backtransformed using standard formulae for the lognormal distribution (Johnson et al. 1994). To calculate covariance components, we used the method described by Searle et al. (1992), in which variance components are estimated separately for each variable and their sum, and the covariance components formed as one half the difference between the variance component of the sum and the sum of the variance components for each variable separately. The sample design allowed us to estimate variance components for all scales and covariance components for the reach, site and plot scales, with the plot covariance component containing contributions from the rock scale.

Stream-scale density

The density at the stream scale is the mean of the smaller-scale densities. The mean periphyton density and grazer density at the stream scale were estimated using ln-transformed and square-root-transformed data, respectively. The means on the natural scale were calculated using standard formulae so as to be free of transformation bias (Miller 1984, Johnson et al. 1994). We used the REML algorithm of Genstat 6.2 (VSN International Ltd, Hemel Hempstead, UK) for all analyses of means and variances because of the hierarchical design described here.

Measuring the scale transition

We measured the scale transition in two ways: quadratic approximation (Eq. 5) and exactly (Eq. 4), by expected value according to the lognormal distribution for periphyton density. To quantify the scale transition for the instantaneous rate of change, the inputs to the quadratic approximation (Eq. 5) were the observed mean periphyton density, $\overline{R}$, and grazer density, $\overline{C}$, at the stream scale, the best-fitting models for periphyton growth, $g(R)$, and grazer foraging, $f(R)$, and their respective derivatives, and the total spatial variance of R and R-C covariance at the rock scale, because this is the scale of density dependence (Chesson 1998*a*). We calculated the exact scale transition for T_g and T_f in Eq. 4 by first finding the expected value of the nonlinear function at the stream scale (e.g., Rice 1995):

$$\overline{F(R)} = \int_0^\infty P(R)F(R)\,dR \qquad (6)$$

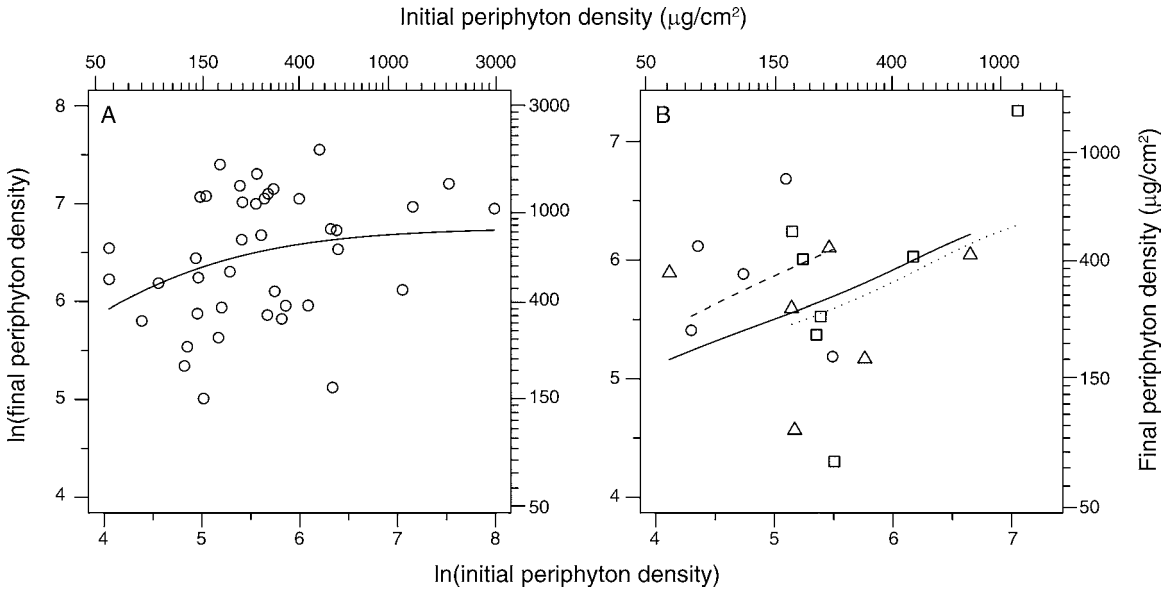

FIG. 1. Initial and final periphyton density, on a natural-log scale, on rocks (A) without grazers and (B) with grazers. Models shown are the best-fitting models for (A) periphyton growth rate, $g(R)$ (the logistic model), and (B) grazer removal rate, $f(R)C$ (the type III model). Panel (B) shows the model for grazer removal rate for average grazer density in the three reaches of the Bimberamala River. Symbols and line styles in panel (B) represent different reaches: triangles and solid line, reach 1; circles and dashed line, reach 2; squares and dotted line, reach 3.

where $P(R)$ is the probability density function of the lognormal distribution with parameters $S^2 = \text{Var}(\ln R)$ and $\overline{\ln R} = \ln \overline{R} - \frac{1}{2}S^2$ (Johnson et al. 1994), and $F(R)$ is the nonlinear function $g(R)$ or $f(R)$. For term T_{fC} of Eq. 4, $\text{Cov}(f(R),C)$ was found exactly using the same method described for $\text{Cov}(R,C)$.

The instantaneous rate of change relates only to the state of the system observed as a snapshot at the time of the experiment. To extend the analyses beyond snapshots to short time scales, we assume that the coefficient of variation, CV, of periphyton density is constant. Then, the spatial variance, $\text{Var}(R)$, is a function of the stream-scale mean such that $\text{Var}(R) = \text{CV}^2\overline{R}^2$, where $\text{CV}^2 = \exp(S^2) - 1$ (Johnson et al. 1994). The covariance cannot be extrapolated in the same way as the variance. Therefore, in the analyses for short time scales that include wide-ranging values for periphyton density, we consider only the contributions of scale transition terms a and b. Nevertheless, terms a and b account for most of the scale transition at the observed stream-scale periphyton density (see *Results*).

Over a short time scale, the dynamics of periphyton density at the stream scale can also be considered in relation to the equilibrium density of periphyton, $\overline{R}^*$, defined as the density attained when periphyton growth at the stream scale is exactly matched by grazer foraging at the stream scale, that is when $d\overline{R}/dt = 0$. Over a time scale of days to weeks, there is effectively a fixed standing crop of grazers at the regional scale but in contrast to grazer dynamics, the dynamics of periphyton are fast over short time scales. Thus, periphyton density averaged over a closed system can approach equilibrium over short time scales and it is useful to examine the properties of this equilibrium.

RESULTS

Nonlinearities: model fits

Consistent with the well-established result of resource competition in biofilms, we found that periphyton growth was nonlinear. Logistic growth (Fig. 1A) was the best fitting of the models defined in Table 1, as it had the lowest AIC (82.1), followed by the resource gradient model (AIC = 83.9). Both linear models had poor fits (AIC; constant accumulation, 87.6; exponential growth, 109.6) compared to the logistic growth model since the AIC difference (ΔAIC) exceeded 4, with essentially no support for the exponential growth model since ΔAIC exceeded 10 (Burnham and Anderson 2002). In contrast to the linear models, both nonlinear models showed no systematic patterns in the residuals, further suggesting that a nonlinear model is essential to describe these data. The SIMEX adjusted parameter estimates for the logistic model were $r = 0.0811$ d^{-1}, $K = 869.6$ μg/cm^2.

It was also clear that periphyton removal rate by grazers was nonlinear. The type III model fitted the data best (AIC 41.1; Fig. 1B), followed by the linear increase model (AIC = 41.5) and the type II model (AIC = 43.5). The saturated model (linear in C only) had the poorest fit (AIC = 50.9; ΔAIC = 9.8), suggesting that the hypothesis of a constant removal rate was unlikely, thus confirming joint nonlinearity in R and C. The SIMEX adjusted parameter estimates for the type III model were $b = 1.15 \times 10^{-5}$ μg^{-2} cm^4 d^{-1}, $h = 1.060$ d. See Appendix C for a detailed table of model fits.

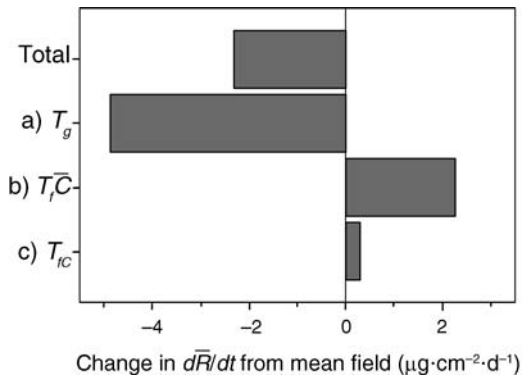

FIG. 2. Contribution of each scale transition term to the total change in the instantaneous rate of periphyton growth, dR/dt, at the stream scale (Eq. 4, terms a–c), estimated from field data. The change shown is relative to the mean-field model.

Spatial variance and covariance components

For periphyton density, most variation occurred at small to medium spatial scales, with similar variance components for ln-transformed density at site (0.1006), plot (0.1360), and rock (0.1483) scales. In contrast to smaller scales, there was almost no variation at the stream (0.0043) or reach (0) scales. See Appendix D for a detailed table of results. The spatial covariance components of periphyton and grazer density, Cov(R,C), and of Cov($f(R)$,C) were small at all scales (Cov(R,C); reach, −821; site, 225; plot plus rock, −180; Cov($f(R)$,C); reach, −0.581; site, −0.003; plot plus rock, 0.289).

Quadratic approximation

Since the best fitting model for periphyton growth rate was the logistic model, a quadratic function, the quadratic expression for scale transition term T_g is exact. The quadratic approximation for scale transition term $T_f\overline{C}$ performed adequately for the best-fitting type III model compared to the exact calculation by expected value (Fig. 3B). For the type III model, the approximation overestimated term T_{fC} by a factor of three compared to the exact calculation. In the analyses that follow (including Figs. 2–4), we present the exact scale transition calculations.

Scale transition for instantaneous rate of change

The scale transition for the instantaneous rate of change of the stream-scale periphyton density was large and negative (Fig. 2). That is, the interaction between nonlinearity and spatial variance in the spatial model reduced $d\overline{R}/dt$ at the stream scale by 98% (from 2.37 to 0.053 μg·cm^{-2}·d^{-1}) compared to the mean-field model. Of the three terms contributing to the scale transition, T_g had the largest effect, followed by $T_f\overline{C}$, with these two scale transition terms having opposing effects (Fig. 2). The positive effect of $T_f\overline{C}$ offset 46% of the negative effect of T_g (Fig. 2). These terms contributed most because the total variance in periphyton density was large and periphyton growth and consumption were nonlinear. The total rock-scale variance on the logarithm scale was 0.385, corresponding to a natural scale CV of 0.685 and spatial variance of 52 215 μg^2/cm^4 for the observed mean periphyton density of 333.5 μg/cm^2. The nonlinearities in periphyton growth and grazer consumption are shown in Fig. 3A and B (rock-scale model). Nonlinearity in periphyton growth was an order of magnitude greater than nonlinearity in the functional response of grazers (logistic $g''(\overline{R}) = -1.87 \times 10^{-4}$, type III $g''(\overline{R}) = -5.40 \times 10^{-6}$).

The contribution of the third scale transition term, T_{fC}, was low compared to the first two terms (Fig. 2), because the covariance between periphyton and grazer density was small. The total covariance, Cov($f(R)$,C), that is, T_{fC} in Eq. 4, was −0.295 μg·cm^{-2}·d^{-1}. This small total covariance was partly due to the weak spatial

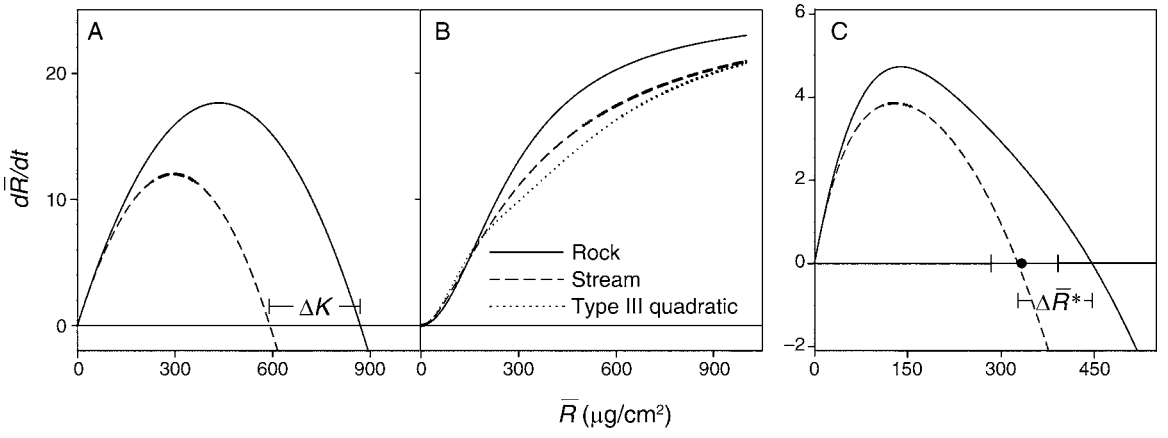

FIG. 3. Comparison of the rock-scale model (mean-field model, solid line) and the exact stream-scale model (dashed line). (A) Logistic periphyton growth, $g(R)$. ΔK represents the change in carrying capacity. (B) Type III grazer removal rate, $f(R)C$. The dotted line is the quadratic approximation for the stream-scale model. (C) Full periphyton–grazer model, $g(R) - f(R)C$. $\Delta\overline{R}^*$ represents the change in equilibrium density. The periphyton density observed at the stream scale is shown with its standard error. The stream-scale models in panels (B) and (C) ignore the small effect of term T_{fC} in Eq. 4.

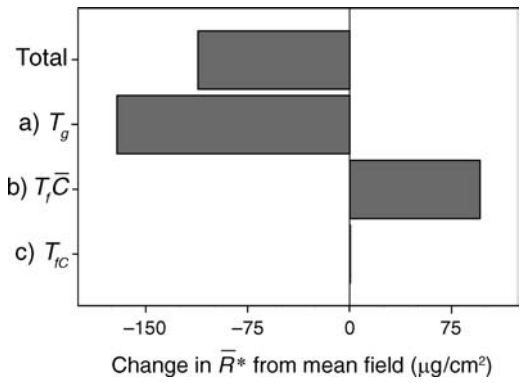

FIG. 4. Contribution of each scale transition term (from Eq. 4) to the total change in the equilibrium density of periphyton at the stream scale. The change shown is relative to the mean-field model. The total change is the combined effect of all three terms. The individual effect of each term is the effect of the term alone without other scale transition terms in the model. In contrast to Fig. 2, the effects here are not additive because the equilibrium is nonlinear in these terms.

association of periphyton and grazer density: the correlations corresponding to the total covariance were $\mathrm{Corr}(R,C) = -0.18$, and $\mathrm{Corr}(f(R),C) = -0.11$. Thus, compared to spatial variation in periphyton density, spatial variation in grazer density contributed little to the scale transition since variation in grazer density contributes only through the covariance term.

Scale transition for short time scales

For periphyton growth without grazers over short time scales, the interaction between nonlinearity and spatial variation is predicted to reduce the growth rate and lower the carrying capacity of periphyton at the stream scale (Fig. 3A). Since the logistic model has a hump-shaped production function, the second derivative is negative. Thus, at all periphyton densities, periphyton growth at the stream scale is reduced compared to the patch scale (Fig. 3A). The maximum growth rate of periphyton at the stream scale is reduced by 32% from 17.6 $\mu g \cdot cm^{-2} \cdot d^{-1}$ to 12.0 $\mu g \cdot cm^{-2} \cdot d^{-1}$ (Fig. 3A). Also, the carrying capacity of periphyton at the stream scale is reduced by 32% from 870 to 592 $\mu g/cm^2$ (Fig. 3A). Apart from these large quantitative changes, the production function for periphyton growth at the stream scale has the same qualitative form as the rock scale (Fig. 3A).

For the rate of grazer consumption, ignoring the small effect of T_{fC}, the stream-scale model predicts that the removal rate will be decreased at high periphyton density ($\overline{R} > 143$ $\mu g/cm^2$) compared to the rock-scale model (Fig. 3B). The magnitude of the scale transition for the removal rate is predicted to be highest at intermediate $\overline{R}$, where the function $f(R)$ is the most nonlinear (Fig. 3B). As well as these quantitative changes, there is a qualitative change in the consumption function at the stream scale: the curve is less pronounced, especially at the inflection point, and resembles more of a type II response.

For the full periphyton–grazer model over short time scales, ignoring the small effect of T_{fC}, the maximum growth rate of periphyton at the stream scale is reduced by 19% to 3.85 $\mu g \cdot cm^{-2} \cdot d^{-1}$, compared to 4.73 $\mu g \cdot cm^{-2} \cdot d^{-1}$ at the rock scale (Fig. 3C). The equilibrium density is reduced by 27% to 327 $\mu g/cm^2$, compared to 447 $\mu g/cm^2$ at the rock scale (Fig. 3C).

Scale transition for the equilibrium density

The equilibrium density was reduced by 25% from 447 $\mu g/cm^2$ in the patch model to 335 $\mu g/cm^2$ in the stream-scale model (Fig. 4). If we can assume the stream-scale density was close to equilibrium at the time of the experiment, the prediction of the stream-scale model was remarkably close to the observed density of 333.5 $\mu g/cm^2$, although the mean-field model was also within the 95% confidence interval for the observed density (241.8, 460.0 $\mu g/cm^2$; Fig. 3C). There was not strong evidence to falsify the assumption of equilibrium, since there was not a significant difference in mean periphyton density at the stream scale between the initial and final samples (grazed rocks, REML, $\chi^2_1 = 0.4204$, $P = 0.52$).

The contribution of the three terms to the scale transition (Eq. 4) of the equilibrium density was very similar to that for the instantaneous rate of change (compare Fig. 4 and Fig. 2). The term T_g had a large negative effect and was opposed by the positive effect of $T_f\overline{C}$ (Fig. 4). Again, the covariance term, T_{fC}, had relatively little effect (Fig. 4).

DISCUSSION

Our field example demonstrates the basic concepts and properties of the scale transition in translating the effects of local scale processes to the scale of the regional population, where local populations are linked by dispersal. By deriving a scale transition model, we identified the component spatial mechanisms that change dynamics at the regional scale. In our field example, the local scale was a rock and the regional scale was the stream. The structure of our model for the stream scale consisted of a mean-field model, representing the local dynamics on a rock, modified by three new terms to correct for the effects of spatial processes (Eq. 4). The new terms in the model were interactions between nonlinearity and spatial variation (Eq. 5). These scale transition terms, which can be thought of as representing spatial mechanisms, were then measured with field data. We confirmed the importance of spatial mechanisms to the dynamics of the system at the stream scale, since we measured scale transition terms with large magnitude. Of the three terms, the largest effect was from the interaction between nonlinear periphyton growth and spatial variation in periphyton density (term T_g), which reduced the instantaneous rate of change in periphyton density (Figs. 2 and 3A). This effect was opposed by the positive effect of the interaction between type III consumption by grazers and spatial variation in periphyton density (term $T_f\overline{C}$; Figs. 2 and 3B) but was

little influenced by the covariance of periphyton and grazer density (term T_{fC}; Fig. 2). The combined effect of the three scale transition terms was to reduce the instantaneous rate of growth of the stream population by 98% compared to the rock-scale populations (Fig. 2) and to reduce the short term equilibrium density by 25% (Figs. 3C and 4).

Studying spatial processes in natural ecological systems is difficult, not least because of the effort required to parameterize and test fully spatial-dynamic models (Steinberg and Kareiva 1997). The scale transition approach offers an alternative to fitting the full details of complex spatial-dynamic models by focusing on the mechanism by which spatial models have important effects, namely the interaction between nonlinearities and spatial variation. This interaction explains the important dynamical outcomes on the larger scale. In this empirical scale transition approach, the effects of complex dispersal modes are measured by their spatial variances and covariances, and their importance evaluated by the magnitude of the terms in which they appear in scale transition equations (e.g., Eq. 5). This focus allows the relative importance of different mechanisms to be assessed quantitatively, and facilitates comparison between different systems and different models. An advantage of the approach is that we can examine spatial mechanisms with relatively little data. Even partial dynamics, such as the short term dynamics examined here, can be explored for mechanistic and biological content. This study was based on one snapshot of spatial structure, yet important spatial mechanisms were revealed.

The dynamics and mechanisms of variation

We measured variances and covariance for a snapshot in time but variances and covariances can also be dynamic. Thus, the scale transition over longer periods than considered here (i.e., months to years) will be different at different times and depend on the dynamics of variation. Ultimately, we need theory for the dynamics of variation. While this area of theory is developing, particularly in the application of moment closure techniques (e.g., Bolker and Pacala 1997, Pacala and Levin 1997, Keeling et al. 2002, Bolker 2003, Law et al. 2003), current models lack major drivers likely to be encountered in nature, such as spatial heterogeneity in the environment (but see Bolker 2003, Snyder and Chesson 2003, 2004), and density-dependent dispersal. Indeed, there are likely to be many processes that contribute to the dynamics of spatial variation, and working them out for specific systems will involve a combination of theory, simulation modeling, behavioral experiments and field studies. This is perhaps one of the greatest challenges in spatial ecology.

For the periphyton–grazer system, the action of grazers is one of the main drivers of spatial variation in periphyton density at small spatial scales as demonstrated by experimental removal of grazers (Fig. 1). Thus, consumption by grazers leads to a system of patches with differing degrees of periphyton regrowth (Nisbet et al. 1998, Richards et al. 2000). However, shallow streams are highly variable environments, with a host of environmental factors that contribute to spatial variation in the biota, including solar radiation, current velocity, water temperature, and disturbance by spates and sedimentation (Allan 1995, Stevenson et al. 1996). Many processes are responsible for spatial variation in this system, as is likely true for all but the simplest of laboratory systems.

A strength of the scale transition approach is that regardless of the complex processes that give rise to spatial variation, we can measure that variation directly. With measurements of variation, we can determine the consequences for dynamics at the regional scale, which come about because of interactions between spatial variation and nonlinearity at the local scale. A full understanding of the mechanisms that generate the dynamics of spatial variation is not necessary to examine the importance of that variation to regional dynamics.

Here we emphasized quantifying the magnitude of scale transition terms to examine the importance of variation to regional dynamics but this empirical approach is readily extended to link the scale transition terms with the longer term dynamics of variances and covariances (Chesson 1996, 1998*a*, *b*). One approach is to empirically determine how variances and covariances vary dynamically as functions of the means. It is straightforward to track the dynamics of variances and covariances using appropriate sampling designs, and empirical studies show that spatial variation often changes systematically with mean density (e.g., Taylor et al. 1988, Clark et al. 1996). Application of the mean-variance relationship to scaling up population dynamics is discussed in Chesson (1998*a*, *b*) and Chesson et al. (2005), where a range of mechanisms that generate such relationships is considered. A fully dynamic system of equations is then constructed by combining scale transition equations with empirical mean-variation functions. This approach is closely related to moment closure methods, in which dynamical equations for variances and covariances are also derived in addition to equations for the means (e.g., Pacala and Levin 1997). In contrast to moment closure methods, which rely on knowing the mechanisms of dispersal in detail, empirical explorations of relations between the moments themselves might often be more tractable for field data.

An aspect of scale transition theory that extends the empirical approach presented here, is how spatial variation on multiple scales contributes to scaling up through an interaction with the spatial scales of nonlinearities (Chesson 1998*a*, *b*). This is especially useful for systems in which different nonlinear processes operate on markedly different scales, or the scales of nonlinearities differ between species. The critical issue for such systems is how variation on different scales propagates to the scales of the nonlinearities, and it is in

this context that quantifying variance components at a range of scales is especially useful.

Acknowledgments

We thank Julian Ash and P. Sam Lake for valuable discussions, and Bruce Barry, John Crockett, Paul Daniel, Kendi Davies, Greg Leidreiter, Eric Melbourne, Alan Muir, and Terry Murphy for assistance with fieldwork. We thank Mercedes Pascual and an anonymous reviewer for comments that improved the manuscript. B. A. Melbourne was supported by an Australian Postgraduate Award and the National Science Foundation Biological Invasions IGERT program, NSF-DGE #0114432.

Literature Cited

Akaike, H. 1992. Information theory and an extension of the maximum likelihood principle. Pages 610–624 *in* S. Kotz and N. Johnson, editors. Breakthroughs in statistics. Springer-Verlag, New York, New York, USA.

Allan, J. D. 1995. Stream ecology: structure and function of running waters. Chapman and Hall, New York, New York, USA.

Bolker, B. M. 2003. Combining endogenous and exogenous spatial variability in analytical population models. Theoretical Population Biology **64**:255–270.

Bolker, B., and S. W. Pacala. 1997. Using moment equations to understand stochastically driven spatial pattern formation in ecological systems. Theoretical Population Biology **52**:179–197.

Bolker, B. M., and S. W. Pacala. 1999. Spatial moment equations for plant competition: understanding spatial strategies and the advantages of short dispersal. American Naturalist **153**:575–602.

Britton, L. J., and P. E. Greeson. 1989. Methods for collection and analysis of aquatic biological and microbiological samples. Revised edition. United States Government Printing Office, Washington, D.C., USA.

Brown, G. G., R. H. Norris, W. A. Maher, and K. Thomas. 2000. Use of electricity to inhibit macroinvertebrate grazing of epilithon in experimental treatments in flowing waters. Journal of the North American Benthological Society **19**: 176–185.

Burnham, K. P., and D. R. Anderson. 2002. Model selection and multimodel inference: a practical information-theoretic approach. Second edition. Springer, New York, New York, USA.

Carroll, R. J., D. Ruppert, and L. A. Stefanski. 1995. Measurement error in nonlinear models. Chapman and Hall, New York, New York, USA.

Chambers, J. M., W. S. Cleveland, B. Kliner, and P. A. Tukey. 1983. Graphical methods for data analysis. Duxbury Press, Boston, Massachusetts, USA.

Chesson, P. 1978. Predator–prey theory and variability. Annual Review of Ecology and Systematics **9**:323–347.

Chesson, P. L. 1981. Models for spatially distributed populations: the effect of within-patch variability. Theoretical Population Biology **19**:288–325.

Chesson, P. 1991. Stochastic population models. Pages 123–143 *in* J. Kolasa and S. T. A. Pickett, editors. Ecological heterogeneity. Springer-Verlag, New York, New York, USA.

Chesson, P. 1996. Matters of scale in the dynamics of populations and communities. Pages 353–368 *in* R. B. Floyd, A. W. Sheppard, and P. J. De Barro, editors. Frontiers of population ecology. CSIRO Publishing, Melbourne, Victoria, Australia.

Chesson, P. 1998*a*. Making sense of spatial models in ecology. Pages 151–166 *in* J. Bascompte and R. V. Solé, editors. Modeling spatiotemporal dynamics in ecology. Landes Bioscience, Austin, Texas, USA.

Chesson, P. 1998*b*. Spatial scales in the study of reef fishes: a theoretical perspective. Australian Journal of Ecology **23**: 209–215.

Chesson, P. 2000. General theory of competitive coexistence in spatially-varying environments. Theoretical Population Biology **58**:211–237.

Chesson, P., M. J. Donahue, B. A. Melbourne, and A. L. Sears. 2005. Scale transition theory for understanding mechanisms in metacommunities. Pages 279–306 *in* M. Holyoak, M. A. Leibold, and R. D. Holt, editors. Metacommunities: spatial dynamics and ecological communities. University of Chicago Press, Chicago, Illinois, USA.

Clark, S. J., J. N. Perry, and E. J. P. Marshall. 1996. Estimating Taylor's power law parameters for weeds and the effect of spatial scale. Weed Research **36**:405–417.

Cook, J. R., and L. A. Stefanski. 1994. Simulation-extrapolation estimation in parametric measurement error models. Journal of the American Statistical Association **89**:1314–1328.

De Jong, G. 1979. The influence of the distribution of juveniles over patches of food on the dynamics of a population. Netherlands Journal of Zoology **29**:33–51.

Doeg, T., and P. S. Lake. 1981. A technique for assessing the composition and density of the macroinvertebrate fauna of large stones in streams. Hydrobiologia **80**:3–6.

Downes, B. J., and M. J. Keough. 1998. Scaling of colonization processes in streams: parallels and lessons from marine hard substrata. Australian Journal of Ecology **23**:8–26.

Downes, B. J., P. S. Lake, and E. S. G. Schreiber. 1993. Spatial variation in the distribution of stream invertebrates: implications of patchiness for models of community organization. Freshwater Biology **30**:119–132.

Flower, R. J. 1985. An improved epilithon sampler and its evaluation in two acid lakes. British Phycological Journal **20**: 109–115.

Graham, A. A., D. J. S. McCaughan, and F. S. McKee. 1988. Measurement of surface area of stones. Hydrobiologia **157**: 85–87.

Hassell, M. P., R. M. May, S. W. Pacala, and P. L. Chesson. 1991. The persistence of host–parasitoid associations in patchy environments. 1. A general criterion. American Naturalist **138**:568–583.

Hershey, A. E., J. Pastor, B. J. Peterson, and G. W. Kling. 1993. Stable isotopes resolve the drift paradox for *Baetis* mayflies in an arctic river. Ecology **74**:2315–2325.

Hill, W. 1996. Effects of light. Pages 121–148 *in* R. J. Stevenson, M. L. Bothwell, and R. L. Lowe, editors. Algal ecology: freshwater benthic ecosystems. Academic Press, San Diego, California, USA.

Hill, W. R., and H. L. Boston. 1991. Community development alters photosynthesis-irradiance relations in stream periphyton. Limnology and Oceanography **36**:1375–1389.

Holling, C. S. 1959. Some characteristics of simple types of predation and parasitism. Canadian Entomologist **91**:385–389.

Ives, A. R. 1988. Covariance, coexistence and the population dynamics of two competitors using a patchy resource. Journal of Theoretical Biology **133**:345–361.

Johnson, N. L., S. Kotz, and N. Balakrishnan. 1994. Continuous univariate distributions. Second edition. John Wiley and Sons, New York, New York, USA.

Keeling, M. J., H. B. Wilson, and S. W. Pacala. 2002. Deterministic limits to stochastic spatial models of natural enemies. American Naturalist **159**:57–80.

Law, R., D. J. Murrell, and U. Dieckmann. 2003. Population growth in space and time: spatial logistic equations. Ecology **84**:252–262.

Lloyd, M. 1967. Mean crowding. Journal of Animal Ecology **36**:1–30.

Melbourne, B. A., and P. Chesson. 2005. Scaling up population dynamics: integrating theory and data. Oecologia **145**:179–187.

Meyer, E. 1989. The relationship between body length parameters and dry mass in running water invertebrates. Archiv für Hydrobiologie **117**:191–203.

Miller, D. M. 1984. Reducing transformation bias in curve fitting. American Statistician **38**:124–126.

Nisbet, R. M., A. M. de Roos, W. G. Wilson, and R. E. Snyder. 1998. Discrete consumers, small scale resource heterogeneity, and population stability. Ecology Letters **1**:34–37.

Nisbet, R. M., S. Diehl, W. G. Wilson, S. D. Cooper, D. D. Donalson, and K. Kratz. 1997. Primary-productivity gradients and short-term population dynamics in open systems. Ecological Monographs **67**:535–553.

Pacala, S. W., and S. A. Levin. 1997. Biologically generated spatial pattern and the coexistence of competing species. Pages 204–232 *in* D. Tilman and P. Kareiva, editors. Spatial ecology: the role of space in population dynamics and interspecific interactions. Princeton University Press, Princeton, New Jersey, USA.

Rice, J. A. 1995. Mathematical statistics and data analysis. Second edition. Duxbury Press, Belmont, California, USA.

Richards, S. A., R. M. Nisbet, W. G. Wilson, and H. P. Possingham. 2000. Grazers and diggers: Exploitation competition and coexistence among foragers with different feeding strategies on a single resource. American Naturalist **155**:266–279.

Ruel, J. J., and M. P. Ayres. 1999. Jensen's inequality predicts effects of environmental variation. Trends in Ecology and Evolution **14**:361–366.

Searle, S. R., G. Casella, and C. E. McCulloch. 1992. Variance components. John Wiley and Sons, New York, New York, USA.

Smock, L. A. 1980. Relationships between body size and biomass of aquatic insects. Freshwater Biology **10**:375–383.

Snyder, R. E., and P. Chesson. 2003. Local dispersal can facilitate coexistence in the presence of permanent spatial heterogeneity. Ecology Letters **6**:301–309.

Snyder, R. E., and P. Chesson. 2004. How the spatial scales of dispersal, competition, and environmental heterogeneity interact to affect coexistence. American Naturalist **164**:633–650.

Stefanski, L. A., and J. R. Cook. 1995. Simulation-extrapolation: the measurement error jackknife. Journal of the American Statistical Association **90**:1247–1256.

Steinberg, E. K., and P. Kareiva. 1997. Challenges and opportunities for empirical evaluation of "spatial theory." Pages 318–332 *in* D. Tilman and P. Kareiva, editors. Spatial ecology: the role of space in population dynamics and interspecific interactions. Princeton University Press, Princeton, New Jersey, USA.

Stevenson, R. J., M. L. Bothwell, , and R. L. Lowe, editors. 1996. Algal ecology: freshwater benthic ecosystems. Academic Press, San Diego, California, USA.

Strahler, A. N. 1952. Hypsometric (area-altitude) analysis of erosional topography. Bulletin of the Geological Society of America **63**:1117–1142.

Taylor, L. R., J. N. Perry, I. P. Woiwood, and R. A. J. Taylor. 1988. Specificity of the spatial power-law in ecology and agriculture. Nature **332**:721–722.

Towers, D. J., I. M. Henderson, and C. J. Veltman. 1994. Predicting dry weight of New-Zealand aquatic macroinvertebrates from linear dimensions. New Zealand Journal of Marine and Freshwater Research **28**:159–166.

Welsh, A. H., A. T. Peterson, and S. A. Altmann. 1988. The fallacy of averages. American Naturalist **132**:277–288.

APPENDIX A

Exact and approximate stream-scale models of periphyton dynamics (*Ecological Archives* E087-087-A1).

APPENDIX B

Derivation of the resource gradient model of periphyton growth. (*Ecological Archives* E087-087-A2).

APPENDIX C

Details of rock-scale model fits (*Ecological Archives* E087-087-A3).

APPENDIX D

Spatial variance components for periphyton (*Ecological Archives* E087-087-A4).